Acta Chemica Scandinavica, 1993: 47: 799–804
Printed in Belgium – all rights reserved

ACTA
CHEMICA SCANDINAVICA
ISSN 0904–213X

Proton Affinity Calculations for MRI Ligands

Rune Fossheim

Nycomed Imaging AS, P.O. Box 4220 Torshov, N-0401 Oslo 4, Norway

Fossheim, R., 1993. Proton Affinity Calculations for MRI Ligands. – Acta Chem. Scand. 47: 799–804.

Molecular modelling techniques and the semiempirical quantum mechanical method MOPAC (AM1) have been used to calculate proton affinities (E_{pa}) for the three basic nitrogens in four polyaminocarboxylate ligands: DTPA (1,4,7-triazaheptane-1,1,4,7,7-pentaacetic acid), DTPA-BMA [1,7-bis(methylcarbamoylmethyl)-1,4,7-triazaheptane-1,4,7-triacetic acid], DTPA-US1 [1,1-bis(methylcarbamoylmethyl)-1,4,7-triazaheptane-4,7,7-triacetic acid] and DTPA-US2 [1,4-bis(methylcarbamoylmethyl)-1,4,7-triazaheptane-1,7,7-triacetic acid]. The calculated E_{pa} values suggest distinctions between the compounds regarding the first protonation step. It is easier to protonate a terminal nitrogen relative to the central nitrogen in DTPA and in DTPA-US2. In DTPA-BMA the situation is the opposite, whereas the E_{pa} values are fairly equal in DTPA-US1. Inductive effects and differences in hydrogen-bonding patterns involving the protonated ligands may explain these findings. The calculated E_{pa}s offer an explanation for the low second protonation constant found in DTPA bis-amides compared with DTPA; protonation of the second nitrogen involves movement of a larger fraction of protons from the central nitrogen to the other terminal nitrogen in the former case. Since the pK_a values are closely tied to the stability of the corresponding Gd-chelates, this gives clues as to how the stability of DTPA-derivatives might be enhanced.

DTPA (1,4,7-triazaheptane-1,1,4,7,7-pentaacetic acid), DTPA-BMA [1,7-bis(methylcarbamoylmethyl)-1,4,7-triazaheptane-1,4,7-triacetic acid] and other aminopolycarboxylates form highly stable Gd(III) ion complexes that are used as chelating agents in magnetic resonance imaging (MRI) techniques.[1,2] The thermodynamic and kinetic stability of such complexes is important for their diagnostic use, since transmetallation is one important source of toxicity.

Replacement of two carboxylate groups in DTPA with amide groups makes the corresponding Gd complex (DTPA-BMA) non-ionic, which is advantageous in terms of osmolality. However, the complex becomes somewhat less stable; $\log K = 22.5$ for GdDTPA[3] and 16.9 for GdDPTA-BMA.[4] It has been shown that $\log K$ is related to the sum of the pK_a values for the different protonation sites in such ligands.[3] Furthermore, the second protonation step in DTPA-bisamides has a significantly lower pK_a value than the corresponding step in DTPA.[5] This pK_a lowering has been ascribed to the different inductive effects of carboxylate and amide groups.

Since pK_a values and protonation mechanisms for these ligands clearly determine the stability of the corresponding Gd complexes, it was decided to examine structure–protonation properties of the ligands shown in Scheme 1 by molecular modelling techniques. Of these ligands, only DTPA-US2 has, to this author's knowledge, not been synthesized.

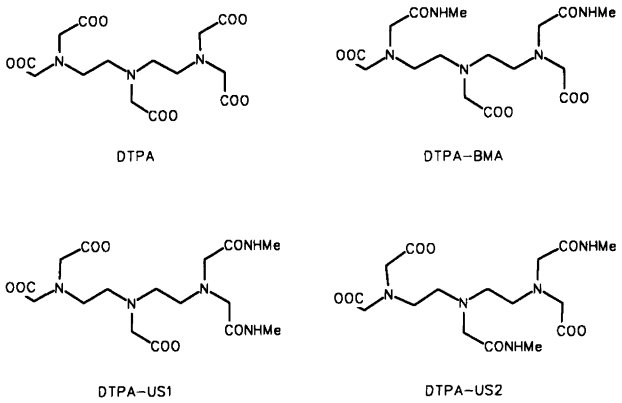

Scheme 1.

Methods

Molecular mechanics calculations and molecular dynamics simulations were performed with the DISCOVER 2.7 software package.[6] Molecular graphics was performed with the INSIGHTII 2.0 programs.[6] Atomic point charges and proton affinities were calculated using the MOPAC 5.0 program package.[7] All calculations were performed on a Silicon Graphics 4D/35 IRIS workstation using the IRIX 3.3.2 operating system.

Proton affinities were calculated for each of the four ligands shown in Scheme 1 using the AM1 Hamiltonian.[8] The proton affinity is defined as $-\Delta H_f$ for reaction (1).

$$B + H^+ = HB^+ \quad (1)$$

The proton affinity E_{pa} is thus taken as in eqn. (2)[9]

$$E_{pa}(B) = -[\Delta H_f(HB^+) - \Delta H_f(B) - \Delta H_f(H^+)] \quad (2)$$

where $\Delta H_f(HB^+)$ and $\Delta H_f(B)$ are the heats of formation of the protonated and unprotonated species, respectively. The heat of formation of H^+ $[\Delta H_f(H^+)]$ is taken as the experimental value (367.2 kcal mol^{-1}),[10] in accordance with previous calculations. E_{pa}s were calculated for the stepwise addition of one proton to the three nitrogens in the four ligands. Protonation of the carboxylate groups was not considered. For the first protonation step, E_{pa} values were calculated for the two (DTPA and DTPA-BMA) or three (DTPA-US1 and DTPA-US2) different nitrogen protonation sites. For the second protonation step only the tautomer with the terminally protonated nitrogen was considered. This is probably the most stable di-protonated tautomeric form, owing to larger charge separation than in the tautomer protonated on neighbouring nitrogens.

The proton affinities were calculated by the following procedure.

1. Starting structures of the unprotonated and protonated forms of the four ligands were built on the graphics screen, using the molecular modelling program INSIGHTII. The main chain was assumed to be *anti* in the starting structures.

2. The starting structures were energy minimized using standard (library) charges and the molecular dynamics/molecular mechanics program DISCOVER. The energy minimizations were performed using a numeric Newton–Raphson minimization method (VA09A), until the gradient was less than 0.03. A distance-dependent dielectric function, $\varepsilon = r_{ij}$, was used.

3. Atomic point charges were calculated for the energy-minimized structures using MOPAC with the MINDO/3 Hamiltonian.

4. The structures were then energy-minimized incorporating the calculated charges and the same minimization procedure as given in section 2.

5. A molecular dynamics simulation was performed at 500 K for each of the structures. The simulation lasted 20 ps, after an initial 5 ps equilibration period. The simulations were run using a 1.0 fs step length and a distance-dependent dielectric function, $\varepsilon = r_{ij}$. Structures observed every ps were selected for energy-minimizations using the minimization procedure described under 2), and subsequently written to disk. This gave a total of 20 energy-minimized structures for each ligand.

6. Heats of formation were calculated for each of the structures having lowest molecular mechanical energy, using MOPAC and the AM1 Hamiltonian.

7. Each of the lowest-energy structures was also used as input coordinates for geometry optimization with the MOPAC program, using the FLEPO geometry optimization procedure and the NOMM keyword.

8. The heats of formation calculated under 6 and 7 were used to determine proton affinities for the molecular mechanics and MOPAC-derived structures according to eqn. (2).

Although for some of the ligands, the molecular dynamics simulations and molecular mechanics calculations identified other conformers that may co-exist in solution, the assumption is made that the calculated E_{pa}s for the lowest energy conformers are representative values for the unprotonated and protonated forms.

Results

Calculated heats of formation for the DISCOVER and MOPAC energy-minimized structures, E_{pa} values and experimental pK_a values for the four ligands are given in Table 1.

Table 1 shows that the E_{pa} values calculated for the MOPAC and DISCOVER energy-minimized structures are fairly consistent, although the heats of formation differ considerably for the DISCOVER and MOPAC geometry-optimized structures they are derived from. The largest differences in the calculated E_{pa} values are for DTPA IA (12.9 kcal mol^{-1}), DPTA IB (9.9 kcal mol^{-1}) and DTPA-US2 II (10.2 kcal mol^{-1}). The remaining differences in the calculated E_{pa}s are all below 5.6 kcal mol^{-1}.

The calculated E_{pa} values are smaller for the second step than the first step for all ligands, as expected from charge considerations and also from experimental pK_a values. However, there is no simple linear relationship between the calculated E_{pa} and experimental pK_a values when comparing all ligands.

The results from the calculations on DTPA suggest that the terminal nitrogens have higher proton affinities than the central nitrogen: 6.0 and 9.0 kcal mol^{-1} for the MM structures and MOPAC structures, respectively. Considering DTPA-BMA the situation is somewhat different. Protonation of the central nitrogen is calculated to be slightly favoured (5.8 and 3.8 kcal mol^{-1}, respectively). For the unsymmetrical bis-amide bearing the amide functions on the terminal nitrogen (DTPA-US1) the proton affinity is clearly lowest for this nitrogen. The E_{pa} values for the central nitrogen and the terminal nitrogen bearing the carboxylate groups are fairly equal. In DTPA-US2 the terminal nitrogen bearing the carboxylate groups has a proton affinity that is 20.8 (MM) and 16.3 (MOPAC) kcal/mol higher than that of the central nitrogen, which in turn is 3.4 (MM) and 6.9 (MOPAC) kcal mol^{-1} higher than that of the central nitrogen bearing one amide group. The rank ordering of E_{pa} for the first protonation step are in accordance with the rank ordering of pK_a values for the first protonation step in DTPA (10.6),[5] DTPA-BMA (9.3)[11] and DTPA-US1 (9.6)[11].

Considering the second protonation step, the ordering of E_{pa} values are in accordance with reported pK_{a2} values; DTPA (8.7),[5] DTPA-BMA (4.4)[11] and DTPA-US1 (5.3)[11]. Considering the three bis-amides, it is found that the proton affinity for the second proton is highest for

Table 1. Calculated heats of formation and proton affinities (E_{pa}) for MRI ligands (kcal mol^{-1}).

Compound	Protonation step/pK_a[a]	ΔH_f/kcal mol^{-1}[b] B	ΔH_f/kcal mol^{-1}[b] HB$^+$	E_{pa}/kcal mol^{-1}[c]
DTPA	IA/10.6	−111.8 (−66.8)	−261.7[d] (−229.5)	517.0 (529.9)
	IB		−270.6 (−235.5)	526.0 (535.9)
	II/8.7	−261.6 (−229.5)	−371.4 (−338.9)	477.0 (476.6)
DTPA-BMA	IA/9.3	−292.5 (−245.8)	−337.3[d] (−293.4)	412.0 (414.8)
	IB		−333.5 (−287.6)	408.2 (409.0)
	II/4.4	−337.3 (−293.4)	−323.0[d] (−278.2)	352.9 (352.0)
DTPA-US1	IA/9.6	−279.3 (−228.5)	−337.2[d] (−291.9)	425.0 (430.6)
	IB		−339.4[d] (−293.8)	427.3 (432.5)
	IC		−320.9[d] (−271.9)	408.8 (410.6)
	II/5.3	−337.1 (−291.9)	−330.8[d] (−284.3)	360.9 (359.6)
DTPA-US2	IA	−286.0[d] (−240.5)	−324.6 (−274.5)	405.8 (401.2)
	IB		−340.9[d] (−295.3)	422.1 (422.0)
	IC		−317.7 (−271.1)	398.9 (397.8)
	II	−324.6 (−274.5)	−327.5[d] (−287.6)	370.1 (380.3)

[a] The protonation steps are: IA, protonation of the central nitrogen; IB, protonation of the terminal nitrogen bearing carboxylate groups; IC, protonation of the terminal nitrogen bearing amide groups; II, protonation of the terminally placed amine nitrogens. The pK_a values were obtained from Ref. 5 and 11. [b] The calculated heats of formation for the conjugated acid (HB$^+$) and base (B) pairs obtained from structures geometry-optimized by MOPAC and molecular mechanics. The latter heats of formation are given in parentheses. [c] The proton affinities derived from the molecular mechanics calculated structures are given in parentheses. [d] In these structures the default convergence criteria in FLEPO were not achieved. However, the gradient norm in all geometry-optimized structures except two was less than 10 kcal mol^{-1} Å^{-2}, and the test for geometry convergence was satisfied in all structures.

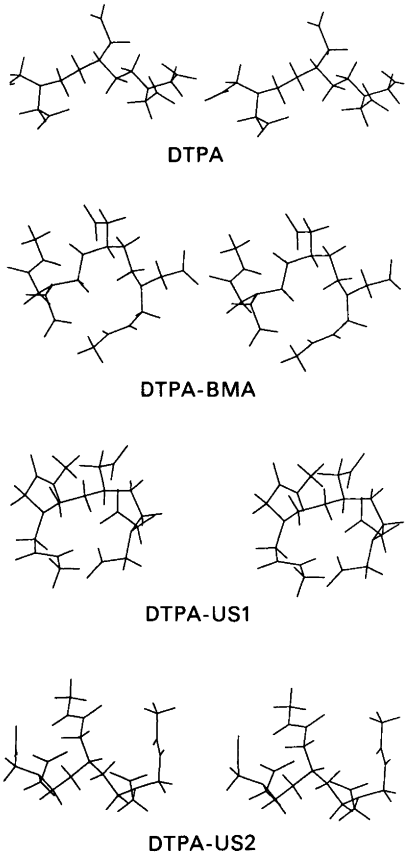

Fig. 1. MOPAC geometry-optimized DTPA, DTPA-BMA, DTPA-US1 and DTPA-US2 ligands protonated on the central nitrogen.

the unsynthesized ligand DTPA-US2 and lowest for DTPA-BMA.

The MOPAC geometry optimized ligands protonated on the central nitrogen (IA) are shown in Fig. 1. The structures protonated on the terminally placed nitrogens bearing the carboxylate groups (IB) and amide groups (IC) are shown in Fig. 2. The di-protonated ligands are shown in Fig. 3.

The adopted conformation and the observed hydrogen-bonding patterns are quite different in the ligands. Comparing the hydrogen-bonding geometries involving the charged nitrogens in DTPA and DTPA-BMA, it is found that, in DTPA protonated on the central nitrogen (IA), there is only one hydrogen bond involving the central carboxylate group. In DTPA protonated terminally (IB) there are two hydrogen bonds formed, both involving the carboxylate groups bonded to the protonated nitrogen. The hydrogen-bonding pattern involving the central *N*(amine) group in DTPA-BMA (IA) is similar to DTPA (IA). However, the hydrogen-bonding pattern involving the terminal *N*(amine) group (IB) is different in DTPA-BMA, since the central carboxylate group is involved in hydrogen bonding. The main chain is slightly 'back-coiled', as may be seen in Fig. 2.

Considering the unsymmetrically substituted amides, DTPA-US1 (IA) has two hydrogen bonds towards the charged NH group, one involving the carboxylate group on the same nitrogen. The tautomer protonated on the terminal nitrogen bearing the two carboxylate groups (IB) forms two hydrogen bonds involving these carboxylate groups. The tautomer protonated on the amide

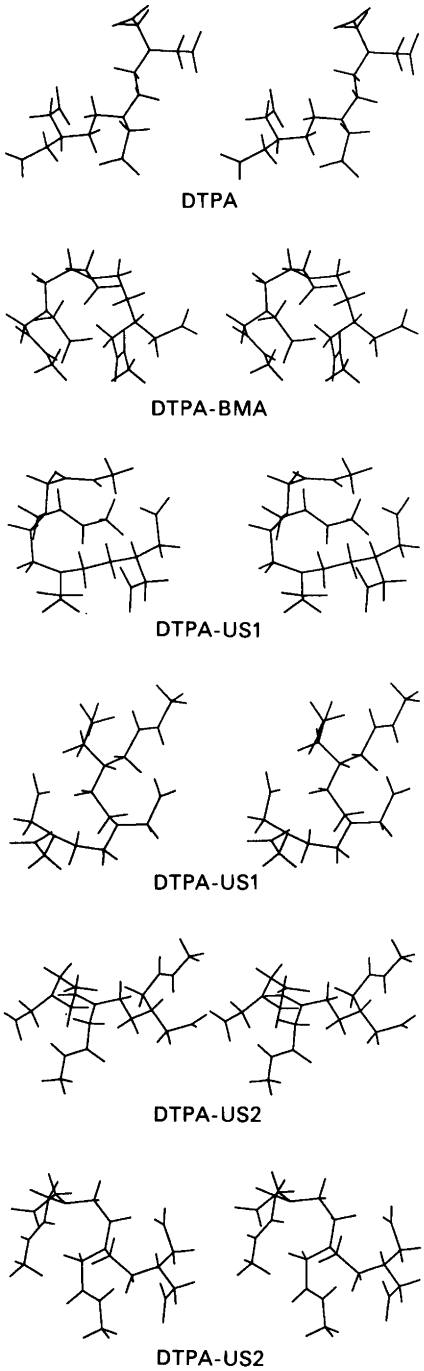

Fig. 2. MOPAC geometry-optimized DTPA, DTPA-BMA, DTPA-US1 and DTPA-US2 ligands monoprotonated on the terminal nitrogens.

side (IC) is not stabilized by hydrogen bonding towards the amide groups. One N–H hydrogen bond is formed towards the centrally placed carboxylate group. The central nitrogen in DTPA-US2 (IA) is not involved in hydrogen bonding towards the central amide group, but towards a terminal carboxylate group. In DTPA-US2 the tautomer protonated terminally on the carboxylate side (IB) is stabilized with two hydrogen bonds towards

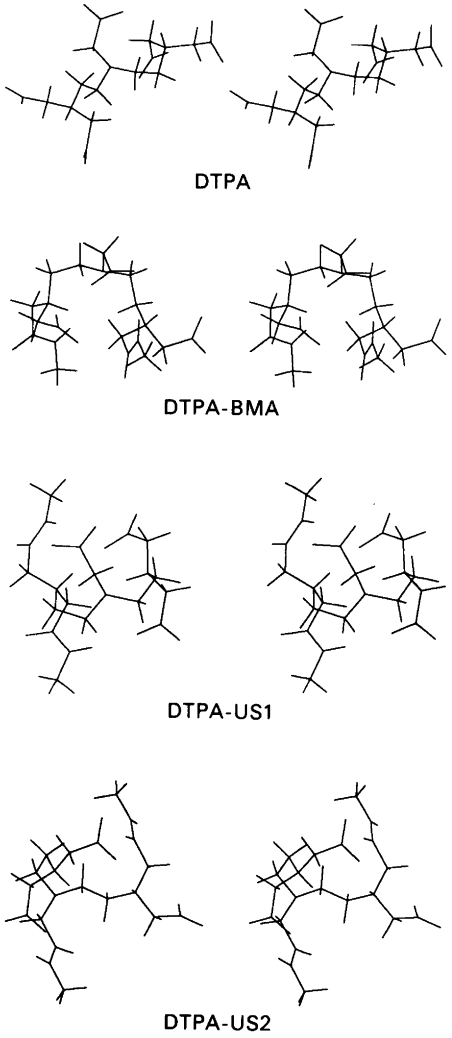

Fig. 3. MOPAC geometry-optimized DTPA, DTPA-BMA, DTPA-US1 and DTPA-US2 ligands diprotonated on the terminal nitrogens.

the carboxylate groups, as is also found in DTPA and DTPA-US1. The tautomer protonated on the terminal amide side is stabilized by two hydrogen bonds: towards the carboxylate group and the amide group on the same nitrogen. In addition to the hydrogen bonds involving the protonated *N*(amine) groups, there are also hydrogen bonds formed between the amide hydrogens and carboxylate groups in the three bis-amides. This may be discerned by inspection of Figs. 1 and 2. Partly as a result of this, the latter ligands have a more globular shape than DTPA.

Considering the di-protonated ligands, the charged N–H groups in DTPA are involved in hydrogen bonds to the four terminal carboxylate groups. In DTPA-BMA only two hydrogen bonds are formed, each involving the terminal carboxylate groups. in DTPA-US1 three hydrogen bonds are formed with the N–H groups, two involving the terminal carboxylate groups and one involving the central carboxylate group. In DTPA-US2 there are four *N*(amine)–H hydrogen bonds formed,

involving the three terminal carboxylate groups and the terminal amide group as acceptors.

Discussion

The calculated proton affinities for DTPA, DTPA-BMA, DTPA-US1 and DTPA-US2 suggest protonation mechanisms that can be compared with results from NMR spectroscopy and potentiometry. Based on NMR and potentiometric measurements it has been suggested that the first protonation step in DTPA and bis-amides like DTPA-BMA involves the central nitrogen. The second protonation step involves protonation of a terminal nitrogen with concerted movement of the first proton to the other terminal nitrogen.[5] The calculated E_{pa} values are not in complete agreement with this scheme, as they suggest a distinction between DTPA and DTPA-BMA. The E_{pa}s suggest that it is easier to protonate the terminal nitrogen in DTPA, whereas protonation of the central nitrogen is slightly favoured in DTPA-BMA. This can be related to the structures and hydrogen-bonding patterns of the monoprotonated species described in the previous section. Whereas the *N*(amine)–H hydrogen-bonding patterns are similar for the centrally protonated tautomer (IA), they are different in the terminally protonated tautomer (IB), since the central carboxylate group is used to stabilize the N–H group in DTPA-BMA (IB). Considering the numerous hydrogen-bonding patterns possible in these compounds and the limited conformational search performed on each ligand, it is difficult to judge the significance of this distinction. However, it may indicate that it is conformationally easier to stabilize a terminal proton by intramolecular hydrogen bonding in DTPA than in DTPA-BMA. Solvation effects, which are not considered in these *in-vacuo* calculations, are expected to make hydrogen bonding less likely between donors and acceptors that are separated by a large number of bonds.

The effects of amide substitution on the calculated E_{pa} values are also apparent for the two unsymmetrically substituted amides, DTPA-US1 and DTPA-US2. The terminal nitrogens bearing the two carboxylate groups have the highest proton affinity, in accordance with more favourable H-bonding interactions. When comparing E_{pa} for protonation at this site with that for protonation at the central nitrogen, it is found that the difference is especially large in DTPA-US2. This ligand is the only one bearing one amide group on the central nitrogen. Stabilization of this tautomeric form is only achieved by hydrogen bonding to a terminally placed carboxylate group.

Considering the hydrogen bonding patterns found in these ligands, it is seen that *N*(amine)–H hydrogen bonding towards the carboxylate groups is highly preferred over the amide oxygens. Hydrogen bonding between *N*(amine)–H and amide oxygens is only observed in DTPA-US2 IC and II. This is probably caused by the fact that carboxylate oxygens are better hydrogen bond donors, owing to higher charge.

It has been suggested that the differences in the measured pK_a values seen in bis-amides like DTPA-BMA as compared with DTPA, is related to the different inductive effects of a carboxylate group and an amide group. One argument against this explanation is that inductive effects are likely to be small when the amide (carboxylate) groups are separated from the protonation site by two σ-bonds. In view of the calculated E_{pa} values discussed above, it is tempting to consider other possible explanations for the observed differences in the pK_a values. The calculated E_{pa}s suggest that the tautomeric equilibrium between the terminally protonated nitrogen and the centrally protonated nitrogen will be shifted more towards the former tautomer in DTPA than in bis-amides like DTPA-BMA. This may be explained by inductive effects and differences in hydrogen-bonding patterns. However, if this is the case, the large drop in the second pK_a value can be explained by the fact that protonation of the second nitrogen will involve movement of a larger fraction of protons from the central nitrogen to the unprotonated terminal nitrogen in DTPA-BMA compared with DTPA. It is assumed that the diprotonated form protonated terminally is most stable. Moving a proton from the central to a terminal nitrogen is less favoured energetically in DTPA-BMA than in DTPA. The experimental pK_{a2} value for DTPA-US1 lies between that for DTPA and DTPA-BMA. This is in accordance with the calculated proton affinities for the second protonation step (II), and it is also in accordance with the calculated difference in E_{pa} for the central and the terminal nitrogens. The latter protonation site is favoured by 6.0 (MM) and 9.0 (MOPAC) kcal mol^{-1} in DTPA, and 1.9 (MM) and 2.3 (MOPAC) kcal mol^{-1} in DTPA-US1. It is disfavoured by 5.8 (MM) and 3.8 (MOPAC) kcal mol^{-1} in DTPA-BMA.

It is interesting to compare the unsynthesized compound DTPA-US2 in this context. It has the highest proton affinity for the second protonation step when comparing the three bis-amides. Furthermore, the difference in proton affinity between the central and the terminal (carboxylate) nitrogen is largest in this compound: 20.8 and 16.3 kcal mol^{-1} in favour of the latter site calculated from the MM and MOPAC structures, respectively. This finding is suggestive of a high second pK_a value.

The E_{pa} values discussed above were calculated without consideration of solvation effects. The solvation energies are presumably quite large for these ligands. However, when comparing E_{pa} for the different protonation sites, only possible differences in solvation energies between the tautomeric forms are relevant for the protonation mechanisms discussed. These solvation effects are judged to be small, in view of the similarity of the tautomers. Solvation effects may partly explain the poor correlation between E_{pa} and pK_a values when considering all four compounds; the calculated E_{pa} values are approximately 100 kcal mol^{-1} larger for DTPA than for the bis-amides. Substitution of two anionic carboxylate groups with neutral amides is likely to result in solvation energy differences for the unprotonated and protonated forms.

Since the sum of the pK_a values is related to the stability of the corresponding Gd-chelates, the above explanation of the differences in experimental pK_a values suggests that the stability of DTPA-derivatives might be increased if the proton affinity of one of the terminal nitrogens can be raised relative to the central nitrogen, thus avoiding proton transfer during the second protonation step. One way of doing this is suggested in DTPA-US2. The calculated E_{pa}s for this compound suggest that protonation of a terminal nitrogen would be even more favoured relative to the central nitrogen than in DTPA. This is indicative of a high second pK_a value and also high complex stability, compared with the bis-amides DTPA-BMA and DTPA-US1. It remains to be determined to what extent this effect might compensate for the beneficial effect of higher ligand charge in DTPA compared with the bis-amides.

References

1. Desreux, J. F. and Barthelemy, P. P. *Nucl. Med. Biol. 15* (1988) 9.
2. Lauffer, R. B. *Chem. Rev. 87* (1987) 901.
3. Cacheris, W. P., Nickle, S. K. and Sherry, A. D. *Inorg. Chem. 26* (1987) 958.
4. Cacheris, W. P., Quay, S. C. and Rocklage, S. M. *Magn. Reson. Imaging. Submitted for publication.*
5. Letkeman, P. and Martell, A. E. *Inorg. Chem. 18* (1979) 1284.
6. Biosym Technologies, Inc. San Diego, CA 92121.
7. Bingham, R. C., Dewar, M. J. S. and Lo, D. H. *J. Am. Chem. Soc. 97* (1975) 1285, 1294, 1302, 1307.
8. Dewar, M. J. S., Zoebisch, E. G., Healy, E. F. and Stewart, J. J. P. *J. Am. Chem. Soc. 107* (1985) 3902.
9. Dewar, M. J. S. and Dieter, K. M. *J. Am. Chem. Soc. 108* (1986) 8075.
10. Stull, D. R., Prophet, J. JANAF *Thermochemical Tables*, NSRDS-NBS37, 1971.
11. The pK_a values for DTPA-BMA and DTPA-US1 were kindly made available by J. Fellman, SALUTAR Inc.

Received September 28, 1992.